

# The Optimization and Characterization of Ultra-Thick Photoresist Films

Warren W. Flack, Warren P. Fan, Sylvia White  
Ultratech Stepper, Inc.  
San Jose, CA 95134

There are an increasing number of advanced lithographic technologies that require photoresist film thickness in excess of twenty microns. For example, suppliers of microprocessors are migrating to flip chip packaging because of bond pad limitations. The flip chip application can require photoresist materials as thick as 125  $\mu\text{m}$  for the bump-bonding step. Another application that requires ultra-thick photoresist films is micromachining (MEMS). Extremely large structure heights are frequently required for micro-electrodeposition of the mechanical components such as coils, cantilevers and valves. These applications can require photoresist in excess of a hundred microns thickness.

The patterning of high aspect ratio structures in these ultra-thick photoresist films is extremely challenging. The aspect ratios easily exceed those encountered in submicron lithography for standard integrated circuit (IC) manufacturing. In addition, the specific photoresist optical properties and develop characteristics degrade the critical dimension (CD) control for these ultra-thick films. The bulk absorption effect of the photoresist reduces the effective dose at the bottom of the film. This effect is exacerbated by the isotropic wet development process which produces sloped profiles. Unlike thin photoresist for IC manufacturing, lithography modeling and characterization are not readily available for ultra-thick photoresist films.

The performance of several commercially available positive and negative ultra-thick photoresists is examined over a thickness range of 20 to 100  $\mu\text{m}$ . This paper is primarily focused on the 25  $\mu\text{m}$  film thickness using both high throughout i-line and gh-line lithography systems optimized for thick film processing. The various photoresists used in this study were selected to represent the full range of available chemistries from multiple suppliers. Basic photoresist characterization techniques for thin films are applied to the ultra-thick photoresist films. The cross sectional SEM analysis and Bossung plots were used to establish relative lithographic capabilities of each photoresist. The trade-offs between the various photoresist chemistries is reviewed and compared with the process requirements for the various applications. A future paper will discuss the capabilities of these same photoresists at both 50 and 100  $\mu\text{m}$  film thicknesses.

**Key Words:** ultra-thick photoresist, MEMS, photoresist characterization, resolution

## 1.0 INTRODUCTION

There are a number of technologies which require the use of thick photoresist films including Micro-Electrical-Mechanical Systems (MEMS), Bump Bonding and Thin Film Heads (TFHs). In semiconductor applications, a photoresist film thickness of less than two microns is typically required for ion implantation or etch processes. While such thin film photoresists have been well characterized and modeled, this information may not adequately describe the performance of thicker photoresist films. Now with growing interest in these other technologies the performance and characterization of ultra-thick photoresists needs to be addressed [1, 2].

In TFH applications a photoresist film of ten microns is frequently required due to the large topography from coil fabrication. The use of a thick photoresist film is the source of many processing issues for this industry. The large topography can cause a variation in the photoresist thickness in excess of 50 percent in the top pole, which in turn effects the critical dimension (CD) control. Slopes in the thick photoresist also reduce the CD control. The higher exposure doses required for these films impact the throughput of the lithography tool [1, 2, 3]. In other applications these same effects are exacerbated because of the even thicker photoresist requirements.

In some MEMS applications, films greater than twenty microns are frequently exposed and developed to produce mechanical structures. These patterns in thick photoresist can have high aspect ratios, depending on the type of structure desired. For certain mechanical structures, such as gears and pumps, the photoresist thickness requirements can easily exceed a hundred microns. There are a number of challenges in imaging thick photoresist that can make it difficult to obtain the required aspect ratios. A CD of 10  $\mu\text{m}$  in a thick 50  $\mu\text{m}$  photoresist has an aspect ratio that would be equivalent to a 0.2  $\mu\text{m}$  line in 1.0  $\mu\text{m}$  of photoresist [4, 5].

The use of photoresist as a sacrificial layer for MEMS processing is very desirable because of the expense of using alternate methods such as glass or metal. Using photoresist decreases the number of processing steps required to produce the molds for these microstructures. However, there may be some process limitations when using photoresist as the sacrificial layer. Currently, some types of fabrication techniques such as LIGA (Lithographie Galvanoformung Abformung) require the sacrificial layer to act as a mold which is then electroplated with metal or deposited with a film. After subsequent processing, the sacrificial layer is then removed to allow the microstructure to form free standing structures.

For some MEMS applications there may be multiple layers which are developed and plated in turn to form step like microstructures. Photoresist may also be used as the mold in these processes. Devices produced using this method include microgears, motors and fiber optic switches. Extra lithography and etch steps are required to pattern the glass or metal layer [4, 5, 6]. In other MEMS applications a thick photoresist layer is used to protect the substrate during the etching of silicon dioxide or metal layers. This layer must often be quite thick because of the harsh etchants required to pattern these materials.

The bump bond applications can also require photoresist film thicknesses in excess of a hundred microns. There are several bump bonding techniques that attach the die bond pads directly to a substrate or package by means of mounds of solder or other die attach material (bump) instead of by wire bonding or tape automated bonding. The thick photoresist film, from 10 to 100  $\mu\text{m}$ , is used to define the location and size of the bump bond. The photoresist is applied, exposed and developed, leaving the bond pads exposed. The solder or die attach material is then deposited. The photoresist is removed and then the metal is reflowed to form the bump [7, 8].

Since the bond pads for bump designs can be located on the active area of the chip, bump bonding can reduce the die size. In addition, the bump bonds can support gigahertz (GHz) speed communication while traditionally wire bonding can only support megahertz (MHz) speeds. This method is more cost effective than traditional vacuum evaporation techniques. The bump method of attaching die is becoming more widespread due to obvious performance advantages [7, 8].

There is a growing interest in using steppers for ultra-thick photoresist applications due to the tighter overlay and improved CD possible with these tools versus that of a contact printer or scanner. The stepper also has the advantage that the focus can be adjusted at various levels into a thick photoresist which will result in improved wall angles and better aspect ratios. Reduction steppers have a narrow band exposure due to the design of their optical systems. However, many of the ultra-thick photoresists are broadband or deep UV sensitive materials. As a result, it is necessary to evaluate ultra-thick photoresist on steppers at different wavelengths to establish best performance.

## 2.0 EXPERIMENTAL METHODS

### 2.1 Reticle Design and Manufacture

The Ultratech 1X reticle used for this study was designed primarily to support easy cross sectional SEM metrology. The reticle consists of two 44 by 22 mm fields, one of each polarity to support both positive and negative photoresists. Each field contains horizontal and vertical line and space pairs of 50, 40, 30, 20, 10, 8.0, 6.0, 4.0 and 2.0  $\mu\text{m}$ . The length of the line and space pairs are designed to facilitate cross sectional SEM analysis. Because of the size of these structures, it is not possible to have a more complete set of line and space pairs on the reticle. The lack of any line sizes between 20 and 10  $\mu\text{m}$  impacted the results of this study and will be discussed in Section 3.0.

The reticle was written on a MEBES 4000 using a high resolution PBS resist. There was no data biasing applied to the design data and CDs were held to within  $\pm 0.03$  of a nominal 2.0  $\mu\text{m}$  chrome line. Reticle CD information was also obtained for all line sizes on both fields to establish the reticle linearity.

## 2.2 Lithography Equipment

Lithography for each photoresist evaluated in this study was performed on both the Ultratech Stepper Saturn Wafer Stepper<sup>®</sup> and the Ultratech Stepper Titan Wafer Stepper<sup>®</sup>. The Saturn stepper and the Titan stepper are based on the 1X Wynne-Dyson lens design employing broadband i-line illumination from 355 to 375 nm and the broadband gh-line illumination from 390 to 450nm, respectively [9]. The specifications of both lithography systems used in this study are shown in Table 1. Exposure uniformity was verified prior to collecting the experimental data and was found to be 1.2 percent across the entire field. Multiple wafers were exposed with a layout consisting of a seven by seven field array as illustrated in Figure 1. Nominal exposure dose was determined by measuring line and space patterns at the specific linewidth of interest with a Hitachi S-7280H metrology SEM. A 40 percent threshold criteria was selected for the determination of the linewidth CD for the negative photoresists while a 0 percent threshold or bottom measurement was selected for the positive photoresists.

## 2.3 Processing Conditions

A number of 150 mm silicon wafers were used for this study. All wafers were vacuum-baked and HMDS primed prior to photoresist coating. Three commercially available ultra-thick photoresist products were used throughout the investigation: THB-521<sup>®</sup> positive photoresist, THB-30LB<sup>®</sup> negative photoresist and SU-825<sup>®</sup> negative photoresist. The THB-521 and THB-30LB are both manufactured by the Japanese Synthetic Rubber company (JSR) while the SU-825 is manufactured by the Microlithography Chemical Corporation (MCC). These photoresists were selected because of the diversity of their photo-chemistries as discussed in Section 3.0. Each photoresist was coated to the 25  $\mu\text{m}$  target thickness using the process and equipment described in Tables 2, 3 and 4 for the JSR THB-521, MCC SU-825 and JSR THB-30LB respectively. Photoresist thickness and uniformity were verified on a Dektak 3030 surface profilometer measurement system.

## 2.4 Data Analysis

Patterned wafers were generated using each of the three photoresists on both the gh-line and i-line lithography systems. Each wafer was visually inspected and measured on the Hitachi S-7280H SEM to determine the minimum linewidth that was resolved with a reasonable process window. This line size was then measured on the S-7280H over the entire focus and exposure matrix as illustrated in Figure 1. The CD data was used to generate Bossung plots for each photoresist on both steppers. A 10 percent CD process control window was calculated from the Bossung plot. This established the focus and exposure values for cross sectional analysis on a Hitachi S-4000 SEM. A total of nine SEM micrographs were made across the process window to show the slope and CD control throughout the process window. These results are discussed in Section 3.0.

### 3.0 RESULTS AND DISCUSSIONS

#### 3.1 JSR THB-521

JSR THB-521 is a positive, novolac-based, broad band photoresist. Its lithographic performance on both the i-line Saturn stepper and the gh-line Titan stepper was evaluated in this study. Cross sectional SEM micrographs of JSR THB-521 on the Saturn and Titan are illustrated in Figure 2 and Figure 3 respectively. In Figures 2a through 2i, the exposure energy was varied from 1,200 mJ/cm<sup>2</sup> to 1,300 mJ/cm<sup>2</sup> and focus offset was varied from -10 μm to +2 μm. In Figures 3a through 3i, the exposure energy was varied from 650 mJ/cm<sup>2</sup> to 850 mJ/cm<sup>2</sup> and total focus offset was varied from -8 μm to -2 μm.

The SEM images show a significant performance difference for the JSR THB-521 in the i-line and the gh-line exposure spectra. Table 5 summarized the performance differences in terms of lithographic parameters. JSR THB-521 demonstrated an 8 μm resolution in the gh-line and 10 μm resolution in the i-line. JSR THB-521 also tends to perform better in the gh-line than that of i-line in terms of exposure latitude. The gh-line focus window beyond the -8 μm to -2 μm range was not investigated.

JSR THB-521 shows a “foot” in the photoresist in both i-line (Figure 2) and gh-line (Figure 3). However, the “foot” in i-line is more pronounced. A “tip-top” shape at the top of the photoresist was observed for both i-line and gh-line and is a characteristic of the photoresist formulation. JSR THB-521 has a relatively low concentration of photoactive compound and is primarily formulated to increase sensitivity in gold bumping package applications. It is the combination of softbake temperature and surface inhibition which causes the appearance of the “tip-top” shape at the top of the photoresist layer.

A close look at the i-line SEM images in Figure 2 also indicates that side wall slopes at -10 μm defocus are more pronounced than at either -4 μm defocus or +2 μm defocus. Within the same focus offset of -10 μm defocus, the side wall profile deteriorates as exposure dose increases as seen in Figure 2a whereas less material develops away as exposure dose decreases as seen in Figure 2g. In contrast, the gh-line SEM images displayed a completely different side wall profile as illustrated in Figure 3. The slopes are concave as compared to the slopes of the i-line images. The degree of concavity increases as exposure dose decreases as well as when focus is shifted toward the positive defocus.

Bossung plots for the i-line and gh-line are shown in Figures 2j and 3j, respectively. The JSR THB-521 results show a large variability in CD as a function of focus for both i-line and gh-line. However, the CD variation in i-line is more pronounced than that in gh-line indicating gh-line has a better process latitude. This is supported by the SEM images shown in Figure 2 and Figure 3 where i-line shows an exposure latitude which is 50 percent less than that of gh-line. A narrow exposure range in the i-line around 1,250 mJ/cm<sup>2</sup> appears to provide about a 12 μm focus range within a ±10 percent CD window. In contrast, the gh-line shows a relatively flat CD response

across focus. Exposures ranging from 600 to 700 mJ/cm<sup>2</sup> provide 6 μm depth of focus within a ±10 percent CD window. The Bossung plots indicate that a positive bias will be required in the i-line and similarly negative bias in the gh-line in order to generate a nominal CD.

In order to use the Bossung plots to determine optimum focus offsets, the focus window has to be extended in both directions to generate a more characteristic Bossung shape. The overall 12 μm focus window was selected based on the configuration of the steppers used in this study. Planned studies on thicker photoresist films will require the stepper to be configured for a larger focus window.

### 3.2 MCC SU-825

MCC SU-825 is a negative, epoxy-type, Shell Chemical EPON<sup>®</sup> resin based photoresist. Its lithographic performance on both the i-line Saturn stepper and the gh-line Titan stepper was evaluated in this study. After an extensive evaluation on the Titan stepper it was determined that MCC SU-825 showed no photo-sensitivity in the gh-line spectrum. Wafers were successfully exposed on the Saturn stepper with the exposure energies varying from 250 mJ/cm<sup>2</sup> to 350 mJ/cm<sup>2</sup> and the focus offsets varied from -10 μm to +2 μm. Cross sectional SEM micrographs are shown in Figure 4. Clearly the total depth of focus for 20 μm lines far exceeds the 12 μm focus window chosen for this study. At the next smallest 10 μm lines, the MCC SU-825 did not show an acceptable process latitude.

A 20 μm equal line and space resolution with vertical side wall was achieved for MCC SU-825 at a 25 μm film thickness. Resolution better than 20 μm is potentially achievable if an appropriate reticle is used. All developed line structures are free of residues. No macroscopic difference in resolution uniformity and side wall profiles was observed across the focus and exposure window used in the study.

The performance reported here is based on the standard immersion techniques for developing the exposed wafers. A limitation was found in developing narrow openings due to the difficulty of refreshing the developer in narrow and deep trenches. Higher aspect ratios may require other techniques such as spray developing to address this issue.

Bossung plots for the 20 μm lines over the 12 μm focus window are shown in Figure 4j. MCC SU-825 shows a very flat CD response across the focus range and all of the CD measurements are within the ±10 percent of the nominal CD limits. In order to generate a more characteristic Bossung shaped curve, the focus window has to be extended in both directions.

### 3.3 JSR THB-30LB

JSR THB-30LB is a negative, acryl-based, photoresist designed for i-line applications. Its lithographic performance on both the i-line Saturn stepper and the gh-line Titan stepper was evaluated in this study. Cross sectional SEM micrographs of JSR THB-30LB on the Saturn are shown in Figure 5 and Figure 6 for the 10 μm and 8 μm resolution respectively. Figure 8 shows 20

$\mu\text{m}$  resolution on the Titan stepper. In Figure 5 the exposure energy varied from  $225 \text{ mJ/cm}^2$  to  $325 \text{ mJ/cm}^2$  and focus offsets varied from  $-10 \mu\text{m}$  to  $+2 \mu\text{m}$ . In Figure 6 the exposure energy varied from  $275 \text{ mJ/cm}^2$  to  $325 \text{ mJ/cm}^2$  and focus offsets were  $-4 \mu\text{m}$  and  $+2 \mu\text{m}$ . In Figure 8 the exposure energy varied from  $1200 \text{ mJ/cm}^2$  to  $1500 \text{ mJ/cm}^2$  and focus offsets varied from  $-10 \mu\text{m}$  to  $+2 \mu\text{m}$ .

Significant performance differences were observed for the JSR THB-30LB between the i-line and the gh-line exposure spectra as illustrated in Figure 5 and Figure 8. Table 6 summarizes the performance differences in terms of lithographic parameters. JSR THB-30LB demonstrated an 8 to  $10 \mu\text{m}$  resolution in the i-line as compared to the  $20 \mu\text{m}$  resolution in the gh-line. The best resolution achieved in the i-line was  $8 \mu\text{m}$  as shown in Figure 6. These results clearly indicate that JSR THB-30LB offers superior performance in the i-line in terms of resolution, although the absolute exposure latitude is better in the gh-line. Vertical side wall profiles were observed for both lithography systems. Resolution better than  $20 \mu\text{m}$  in the gh-line is possible if another reticle with structures between  $20$  and  $10 \mu\text{m}$  is utilized.

Bossung plots for the i-line and gh-line are shown in Figures 5j and 8j respectively. The JSR THB-30LB results show a flat CD distribution as a function of focus for both i-line and gh-line and fall within the  $\pm 10$  percent CD window. This indicates that negative JSR THB-30LB photoresist has better control in exposure latitude than the positive, JSR THB-521 photoresist. The Bossung plots also indicate that a negative bias will be required in the i-line lithography in order to generate a nominal CD.

The normalized film retention curve in gh-line is shown in Figure 7. The after develop film thickness was measured at  $-4 \mu\text{m}$  focus over the  $+10$  to  $-60$  percent range of exposure doses. A value of 1 indicates that the film thickness is the same as the pre-develop thickness. The highest value of 0.95 is observed at  $1,300$  to  $1,350 \text{ mJ/cm}^2$  exposure dosage, which closely matches the nominal dose from the Bossung curve in Figure 8j.

## 4.0 CONCLUSIONS

Standard photoresist characterization techniques have been applied to three commercially available thick photoresist products, JSR THB-521, MCC SU-825 and JSR THB-30LB. Cross sectional SEM analysis and Bossung plots were used to establish relative lithographic capabilities of each photoresist. The trade-offs between the various photoresist chemistries were reviewed and compared with the process requirements for the various applications.

This paper has explored the performance of all three materials for high-aspect-ratio applications on the Ultratech Saturn and Titan family steppers. A  $25 \mu\text{m}$  film thickness was investigated in this study. A future paper will discuss the capabilities of these same photoresists at both  $50$  and  $100 \mu\text{m}$  film thicknesses.

A summary of recommended lithographic applications for the three thick photoresist products is shown in Table 7. Note that a resolution of better than 20  $\mu\text{m}$  for the SU-825 is possible if a reticle with appropriate linesizes is utilized. It is also possible that the performance of the three photoresist products can be significantly improved in terms of aspect-ratio when explored in an even thicker film regime.

## 5.0 REFERENCES

1. Flores, Flack, Tai, "An Investigation of the Properties of Thick Photoresist Films," *Advances in Resist Technology and Processing XI Proceedings*, SPIE **2195**, 1994.
2. Flores, Flack, Tai, Mack "Lithographic Performance in Thick Photoresist Applications," *OCG Microlithography Seminar*, Interface '93 Proceedings, 1993.
3. Gau, "Photolithography for Integrated Thin-Film Read/ Write Heads," *Optical/ Laser Microlithography II Proceedings*, SPIE **1088**, 1989.
4. Cui, Lawes, "A New Sacrificial Layer Process for the Fabrication of Micromechanical Systems," *Journal of Micromechanics and Microengineering*, **7**(3), September 1997.
5. Lehr, "New Extensions of LIGA Technology," *Micromachine Devices*, November 1996.
6. Conedera, Fabre, Dilhan, "A Simple Optical System to Optimize a High Depth to Width Aspect Ratio Applied to a Positive Photoresist Lithography Process," *Journal of Micromechanics and Microengineering*, **7**(3), September 1997.
7. Cheang, Staud, Newman, "A Low Cost Lithography Process for Flip Chip Applications in Advanced Packaging Industry," *Advanced Manufacturing Technologies Seminar*, 1997.
8. Lau, "Next Generation Low Cost Flip Chip Technologies," *46th Electronic Components & Technology Conference*, 1996.
9. Flores, Flack, Dwyer, "Lithographic Performance of a New Generation i-line Optical System," *Optical/Laser Lithography VI Proceedings*, SPIE **1927** (1993).

Parameter	Titan	Saturn
Reduction factor	1X	1X
Wavelength (nm)	390-450	355-375
Numerical Aperture (NA)	0.32	0.365
Partial Coherence ( $\sigma$ )	0.50	0.44
Wafer plane Irradiance ( $\text{mW}/\text{cm}^2$ )	1200	700

**Table 1:** Specifications of the lithography systems used in this study.

Process Step	Parameters	Equipment
Adhesion Promotion	HMDS vapor prime	YES LP-3 Oven
Photoresist Coat	Static dispense: 0 rpm for 5 seconds Spread: 1000 rpm for 10 seconds Spin: 2000 rpm for 1 second	Solitec 5110C Coater
Softbake	420 seconds at 120°C, Hard-contact	Solitec VBS-200
Coolbake	30 minutes at room temperature	
Post Exposure Bake	None	Solitec VBS-200
Develop	JSR PD523AD at 25°C 210 seconds immersion with mild agitation	

**Table 2:** Process conditions for JSR THB-521 photoresist.

Process Step	Parameters	Equipment
Adhesion Promotion	HMDS vapor prime	YES LP-3 Oven
Photoresist Coat	Static dispense: 0 rpm for 5 seconds Spread: 1000 rpm for 10 seconds Spin: 2500 rpm for 30 seconds	Solitec 5110C Coater
Softbake	300 seconds at 95°C, Hard-contact	Solitec VBS-200
Coolbake	30 minutes at room temperature	
Post Exposure Bake	90 seconds at 50°C, followed by 90 seconds at 95°C	Solitec VBS-200
Develop	Shipley XP-9520 at 25°C 300 seconds immersion with mild agitation	

**Table 3:** Process conditions for MCC SU-825 photoresist.

Process Step	Parameters	Equipment
Adhesion Promotion	HMDS vapor prime	YES LP-3 Oven
Photoresist Coat	Static dispense: 0 rpm for 5 seconds Spread: 2000 rpm for 10 seconds Spin: 3000 rpm for 1 second	Solitec 5110C Coater
Softbake	300 seconds at 90°C, Hard-contact	Solitec VBS-200
Coolbake	30 minutes at room temperature	
Post Exposure Bake	None	Solitec VBS-200
Develop	0.5% TMAH at 25°C 120 seconds immersion with mild agitation	

**Table 4:** Process conditions for JSR THB-30LB photoresist.

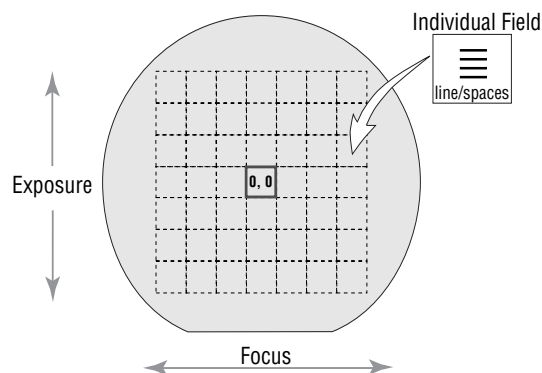


**Figure 1:** Wafer layout for the focus and exposure test matrix.

Lithographic Parameters	i-line	gh-line
Resolution	10 $\mu\text{m}$	8 $\mu\text{m}$
Nominal Dose	1250 $\text{mJ}/\text{cm}^2$	750 $\text{mJ}/\text{cm}^2$
Exposure Latitude	1200-1300 $\text{mJ}/\text{cm}^2$	650-850 $\text{mJ}/\text{cm}^2$
Focus Latitude	-10 to +2 $\mu\text{m}$	-8 to -2 $\mu\text{m}$
Required Bias	Positive bias	Negative bias

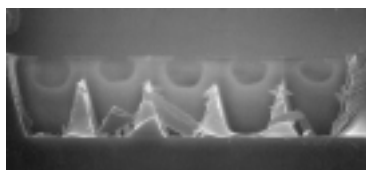
**Table 5:** Summary of JSR THB-521 lithographic performances in i-line and gh-line.

Lithographic Parameters	i-line	gh-line
Resolution	10 $\mu\text{m}$	20 $\mu\text{m}$
Nominal Dose	275 $\text{mJ}/\text{cm}^2$	1350 $\text{mJ}/\text{cm}^2$
Exposure Latitude	225-325 $\text{mJ}/\text{cm}^2$	1200-1500 $\text{mJ}/\text{cm}^2$
Focus Latitude	-10 to +2 $\mu\text{m}$	-10 to +2 $\mu\text{m}$
Required Bias	Negative bias	No bias

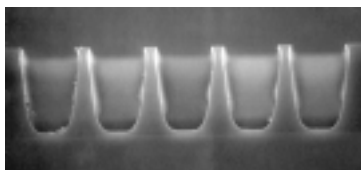
**Table 6:** Summary of JSR THB-30LB lithographic performances in i-line and gh-line.

Photoresists	JSR THB-521	JSR THB-30LB	MCC SU-825
Lithographic Equipment	Titan	Saturn	Saturn
Resolution	8 $\mu\text{m}$	8-10 $\mu\text{m}$	20 $\mu\text{m}$
Nominal Dose	750 $\text{mJ}/\text{cm}^2$	275 $\text{mJ}/\text{cm}^2$	300 $\text{mJ}/\text{cm}^2$
Exposure Latitude	650-850 $\text{mJ}/\text{cm}^2$	225-325 $\text{mJ}/\text{cm}^2$	250-350 $\text{mJ}/\text{cm}^2$
Focus Latitude	-8 to -2 $\mu\text{m}$	-10 to +2 $\mu\text{m}$	-10 to +2 $\mu\text{m}$
Required Bias	Negative bias	Positive bias	No bias

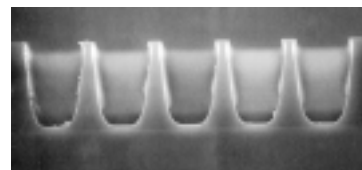
**Table 7:** Recommended lithographic applications on Ultratech steppers in 25  $\mu\text{m}$  films for JSR THB-521, JSR THB-30LB, and MCC SU-825 photoresists.



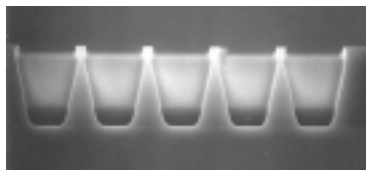
(a) Exposure = 1300 mJ/cm<sup>2</sup>  
Focus = - 10 µm



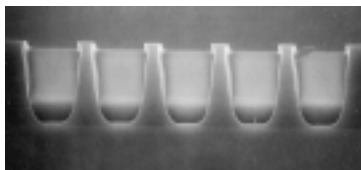
(b) Exposure = 1300 mJ/cm<sup>2</sup>  
Focus = - 4 µm



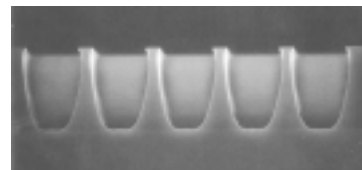
(c) Exposure = 1300 mJ/cm<sup>2</sup>  
Focus = +2 µm



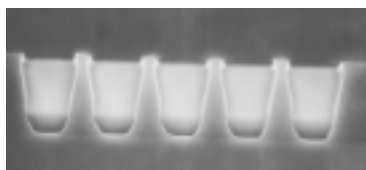
(d) Exposure = 1250 mJ/cm<sup>2</sup>  
Focus = - 10 µm



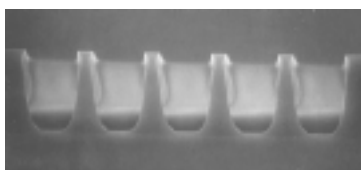
(e) Exposure = 1250 mJ/cm<sup>2</sup>  
Focus = - 4 µm



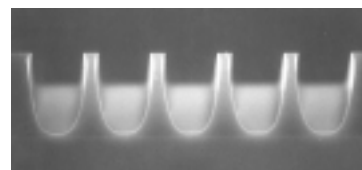
(f) Exposure = 1250 mJ/cm<sup>2</sup>  
Focus = +2 µm



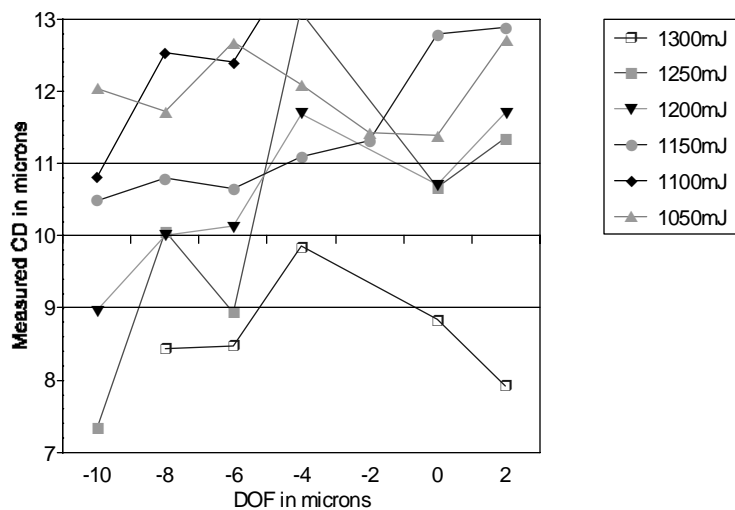
(g) Exposure = 1200 mJ/cm<sup>2</sup>  
Focus = - 10 µm



(h) Exposure = 1200 mJ/cm<sup>2</sup>  
Focus = - 4 µm

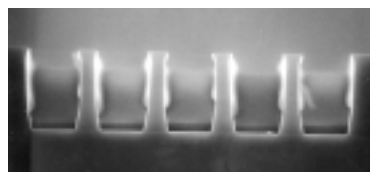


(i) Exposure = 1200 mJ/cm<sup>2</sup>  
Focus = +2 µm

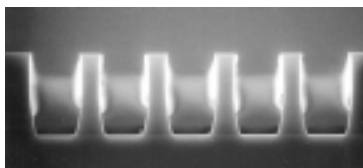


(j) Bossung plot with ± 10 percent control limits

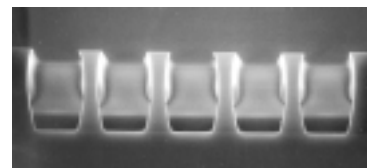
**Figure 2:** Focus and exposure matrix of JSR THB-521 exposed at i-line. The lines and spaces are 10 µm. The SEM micrographs are at 1.0K magnification.



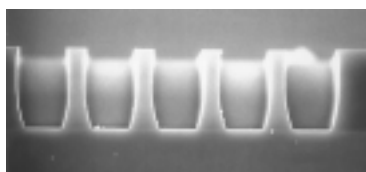
(a) Exposure = 850 mJ/cm<sup>2</sup>  
Focus = - 8 µm



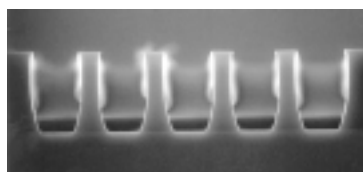
(b) Exposure = 850 mJ/cm<sup>2</sup>  
Focus = - 5 µm



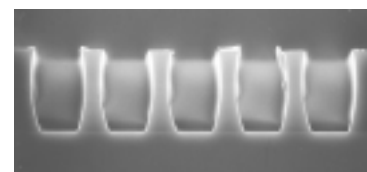
(c) Exposure = 850 mJ/cm<sup>2</sup>  
Focus = -2 µm



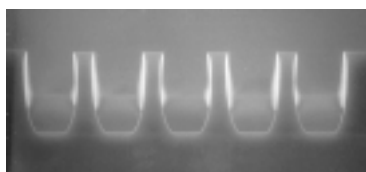
(d) Exposure = 750 mJ/cm<sup>2</sup>  
Focus = - 8 µm



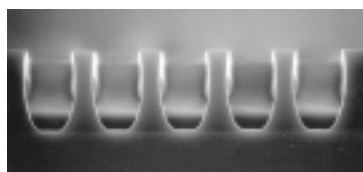
(e) Exposure = 750 mJ/cm<sup>2</sup>  
Focus = - 5 µm



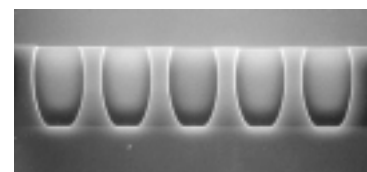
(f) Exposure = 750 mJ/cm<sup>2</sup>  
Focus = -2 µm



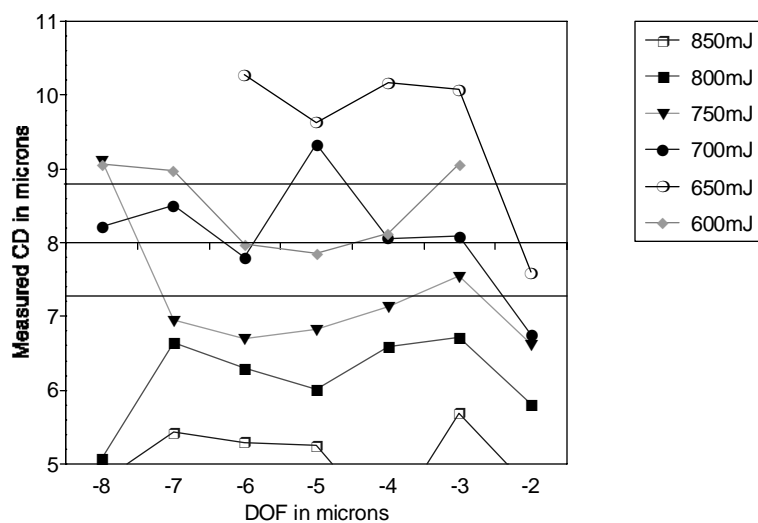
(g) Exposure = 650 mJ/cm<sup>2</sup>  
Focus = - 8 µm



(h) Exposure = 650 mJ/cm<sup>2</sup>  
Focus = - 5 µm

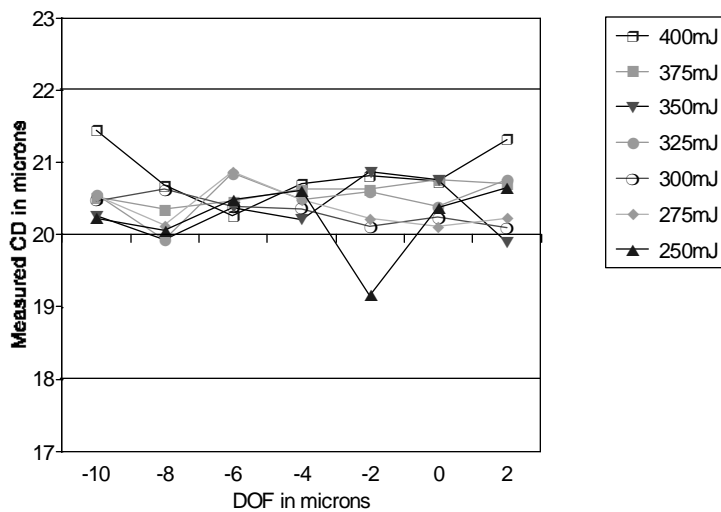
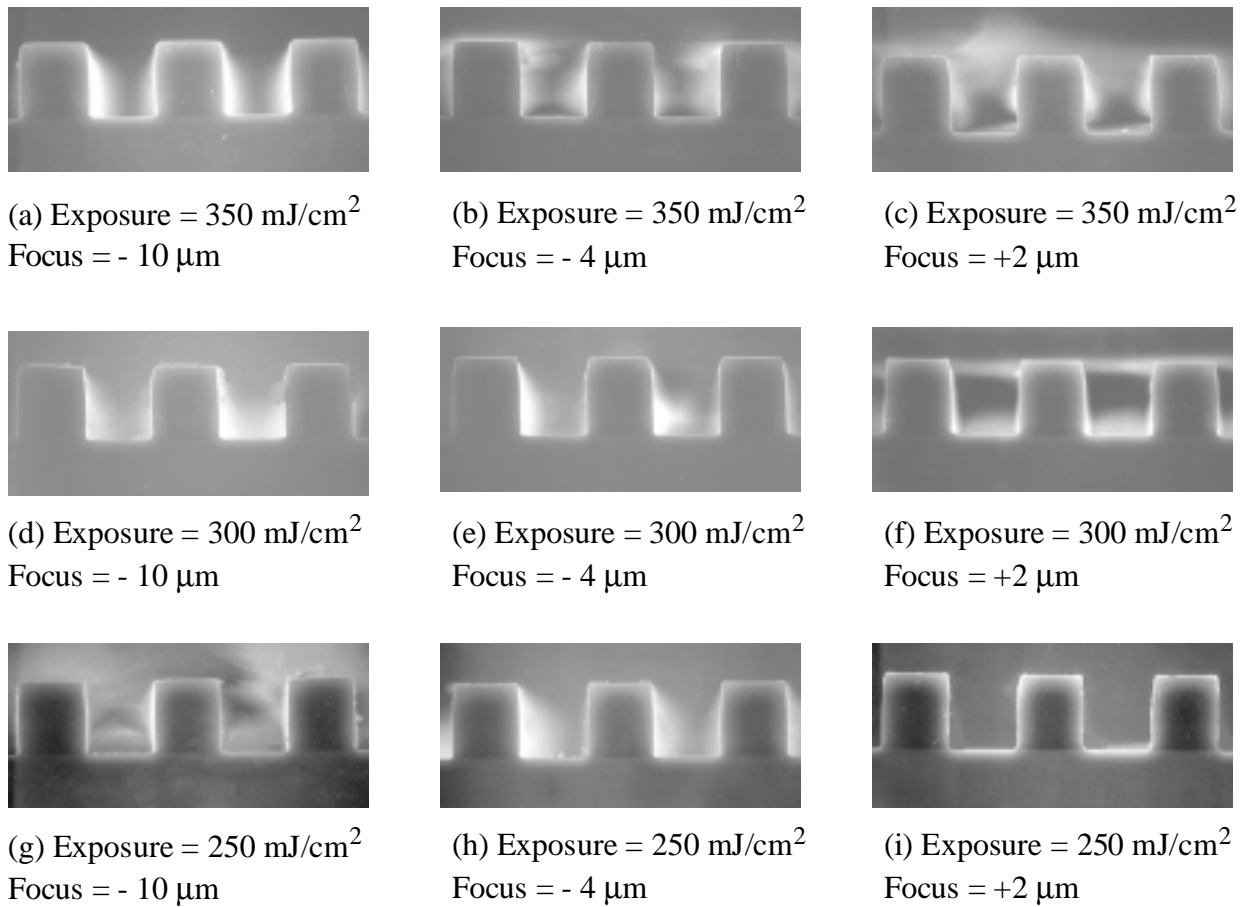


(i) Exposure = 650 mJ/cm<sup>2</sup>  
Focus = -2 µm



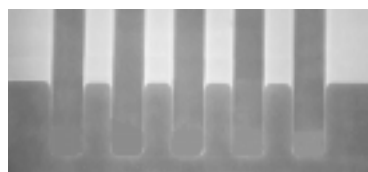
(j) Bossung plot with  $\pm 10$  percent control limits

**Figure 3:** Focus and exposure matrix of JSR THB-521 exposed at gh-line. The lines and spaces are 8 µm. The SEM micrographs are at 1.0K magnification.

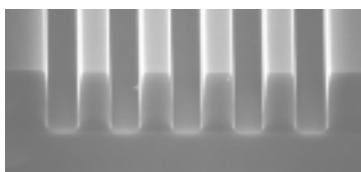


(j) Bossung plot with ± 10 percent control limits

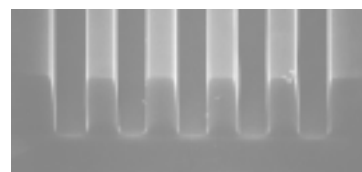
**Figure 4:** Focus and exposure matrix of MCC SU-825 exposed at i-line. The lines and spaces are 20 μm. The SEM micrographs are at 1.0K magnification.



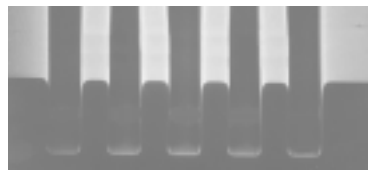
(a) Exposure = 325 mJ/cm<sup>2</sup>  
Focus = - 10 μm



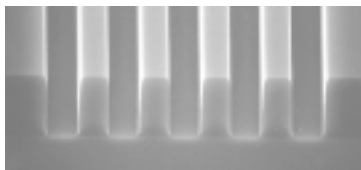
(b) Exposure = 325 mJ/cm<sup>2</sup>  
Focus = - 4 μm



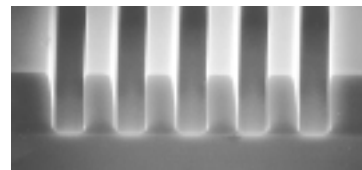
(c) Exposure = 325 mJ/cm<sup>2</sup>  
Focus = +2 μm



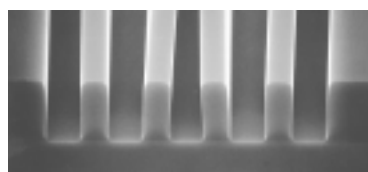
(d) Exposure = 275 mJ/cm<sup>2</sup>  
Focus = - 10 μm



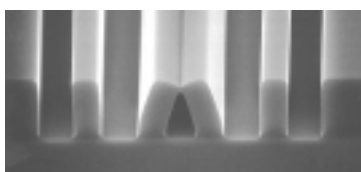
(e) Exposure = 275 mJ/cm<sup>2</sup>  
Focus = - 4 μm



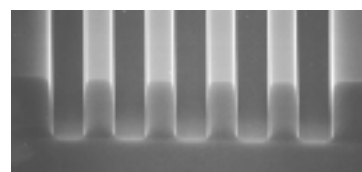
(f) Exposure = 275 mJ/cm<sup>2</sup>  
Focus = +2 μm



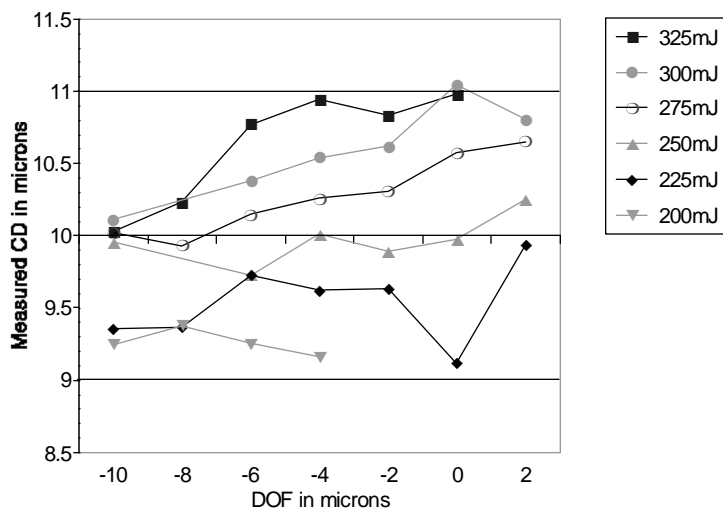
(g) Exposure = 225 mJ/cm<sup>2</sup>  
Focus = - 10 μm



(h) Exposure = 225 mJ/cm<sup>2</sup>  
Focus = - 4 μm

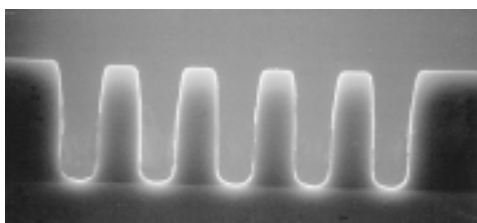


(i) Exposure = 225 mJ/cm<sup>2</sup>  
Focus = +2 μm

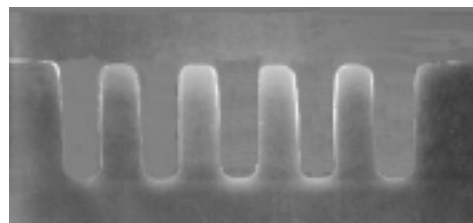


(j) Bossung plot with ± 10 percent control limits

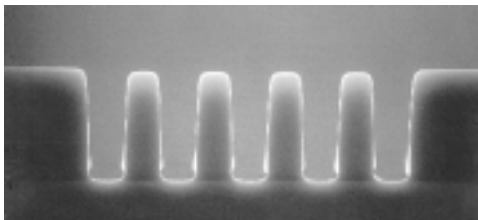
**Figure 5:** Focus and exposure matrix of JSR THB-30LB exposed at i-line. The lines and spaces are 10 μm. The SEM micrographs are at 1.0K magnification.



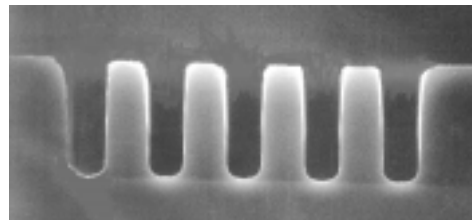
(a) Exposure =  $325 \text{ mJ/cm}^2$   
Focus =  $-4 \mu\text{m}$



(b) Exposure =  $325 \text{ mJ/cm}^2$   
Focus =  $+2 \mu\text{m}$



(c) Exposure =  $275 \text{ mJ/cm}^2$   
Focus =  $-4 \mu\text{m}$



(d) Exposure =  $275 \text{ mJ/cm}^2$   
Focus =  $+2 \mu\text{m}$

**Figure 6:** Focus and exposure matrix of JSR THB-30LB exposed at i-line. The lines and spaces are  $8 \mu\text{m}$ . The SEM micrographs are at 1.0K magnification.

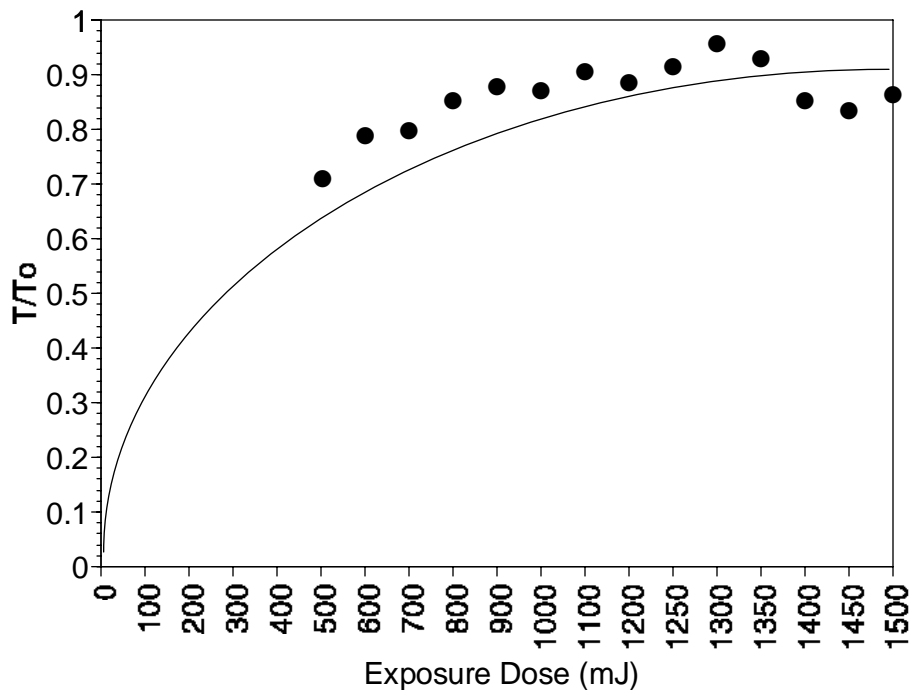
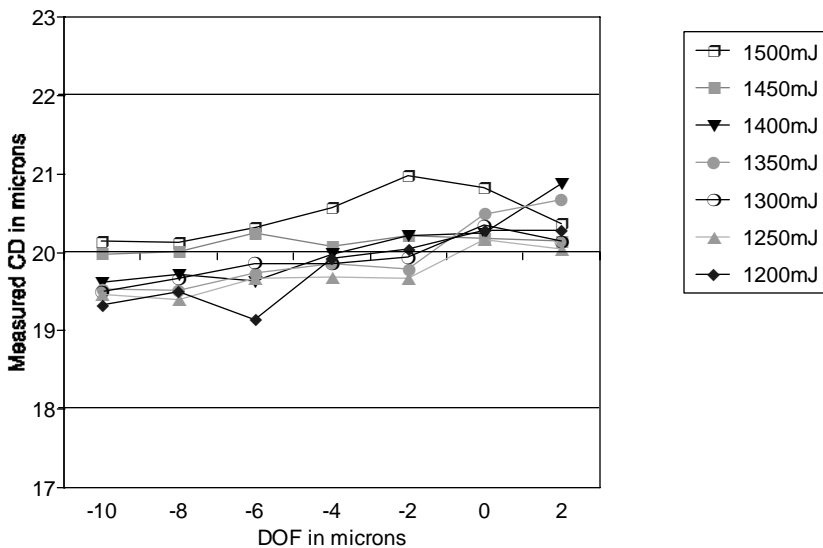
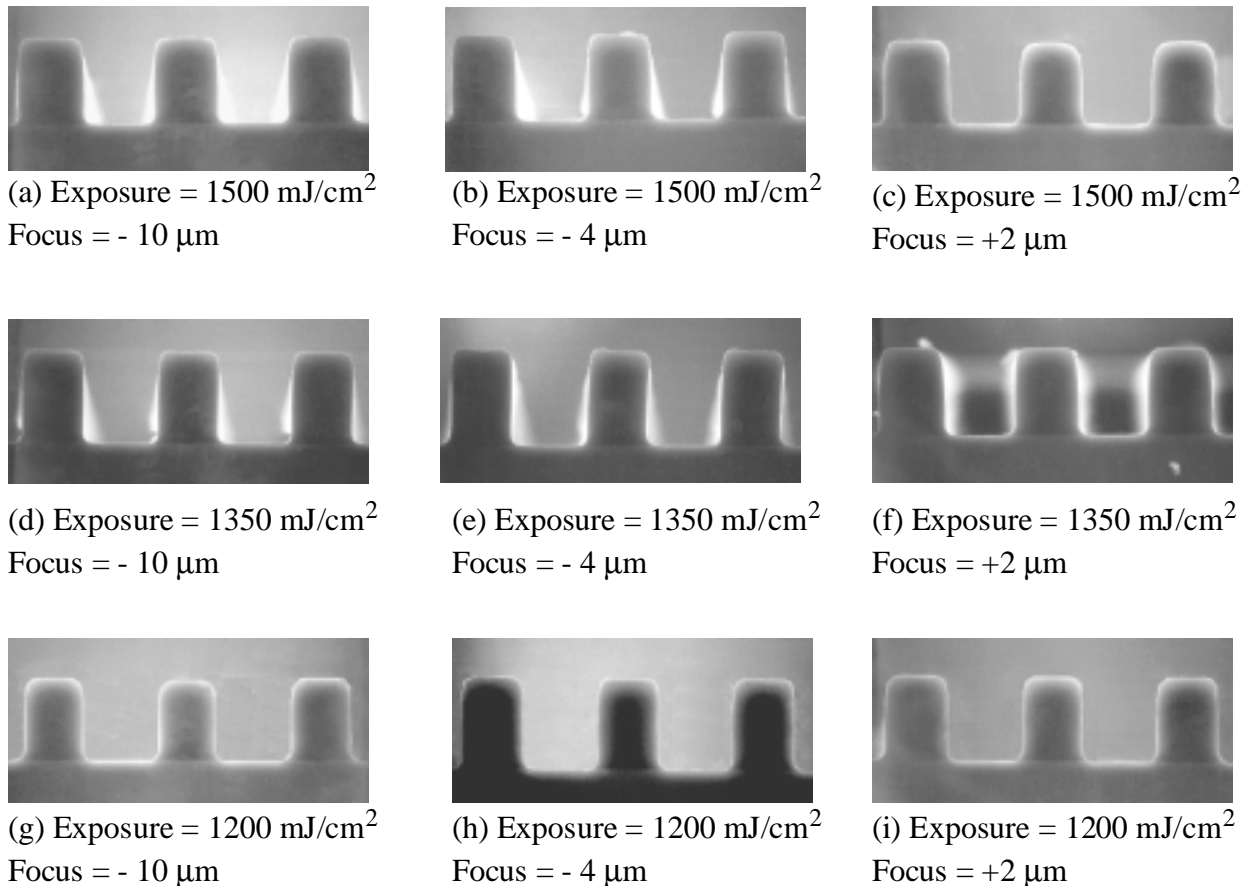


**Figure 7:** Film retention curve for JSR THB-30LB exposed at gh-line. The normalized film retention is plotted against the exposure dose. A value of 1 indicates that the film thickness is the same as the pre-develop thickness.



(j) Bossung plot with ± 10 percent control limits

**Figure 8:** Focus and exposure matrix of JSR THB-30LB exposed at gh-line. The lines and spaces are 20 μm. The SEM micrographs are at 1.0K magnification.